Development of Equipment and Technology for Precision Air-Plasma Cutting of Plate Steel

S. V. Anakhov[a], * (ORCID: 0000-0003-1460-6305), **B. N. Guzanov**[a], ** (ORCID: 0000-0001-5698-0018), and **A. V. Matushkin**[b], *** (ORCID: 0000-0001-7309-1618)

[a] *Russian State Professional Pedagogical University, Ekaterinburg, 620012 Russia*
[b] *Ural Federal University, Ekaterinburg, 620002 Russia*
*e-mail: sergej.anahov@rsvpu.ru
**e-mail: boris.guzanov@rsvpu.ru
***e-mail: 227433@yandex.ru

Abstract—This work studies the structure of cutting seams obtained after cutting steel 09G2S with a new PMVR-5.3 narrow-jet plasma torch which has a number of design features in the gas dynamic stabilization system (GDS) of plasma arc. To increase the efficiency of the GDS in the PMVR-5.3 plasma torch, a symmetrical input of plasma-forming gas (PFG) into the flow division system and a gas-dynamic flow stabilizer using two (forming and stabilizing) swirlers with a variable number of swirl channels were used. It is shown that the achieved advantage in the GDS efficiency makes it possible to obtain a high cutting quality on steel 09G2S with a thickness of 40 mm at high productivity and lower energy costs. Analytical methods have proven a high precision degree of cutting with the new torch—a small cut width, no melting and rounding of the upper edge, as well as a grate in the lower part of the cut and splashes in its upper part, almost zero angular deviation, minimal surface microtopography values and width of the thermal impact zone. A metallographic analysis and a hardness measurement detected three subzones in the thermal impact zone with significant structural changes in two of them. Several factors are noted influencing the revealed structuring changes as well as the changes in the elemental composition of the cutting seam surface layer revealed during the X-ray spectral analysis. Attention is drawn to the surface microtopography after plasma cutting. This topography is commensurate by all quality indicators with the postmilling machining of the surface and corresponds to the second class of surface cleanliness. It is proven that the new narrow-jet plasma torch allows performing a high-quality cutting of plate steel with thicknesses up to 40 mm or more. However, the welding of blanks without pre-machining can be carried out at a cut thickness of no more than 20 mm.

Keywords: plasma torch, design, thermal impact zone, structure transformation, defects, quality, efficiency

INTRODUCTION

The development of modern blank piece production during the fabrication of critical welded metal structures and several other machine building items is intended, first of all, for upgrading primary rolled stock processing technologies. The appropriate choice of such technologies largely determines the subsequent number of necessary operations and, as a consequence, ultimate prime cost of fabricated products. One of the most significant technologies, the requirements on which are constantly toughened, is the cutting of steel sheets of various shapes with a high quality and precision of cutting, which is most often hard to make by conventional processing techniques.

Currently, the most promising technologies for these purposes are air-plasma cutting methods [1—3]. According to several authors, plasma cutting is a no-

alternative technology in blank and welding production for handling various metallic materials of medium and large thicknesses in a range of 10—50 mm [4—6]. In comparison against the mechanical, laser, hydroabrasive, and gas methods of metal handling, plasma cutting allows achieving a required quality within the mentioned thickness range at high productivity and very low specific prime cost of the process [7—9]. At the same time, it is necessary to consider that the competitive advantages of plasma cutting are achievable only by using modern high-efficiency plasmatrons known as the main elements of this production process. However, according to the analysis of the Russian market for plasmatronic equipment, the Russian-designed products are inferior by most significant technical parameters to the plasmatrons from the best foreign producers (Hypertherm, Kjellberg, Messer-Greisheim and some others) [10—12]. Therefore, spe-

Fig. 1. PMVR-5.3 plasma torch for high-precision air-plasma metal cutting.
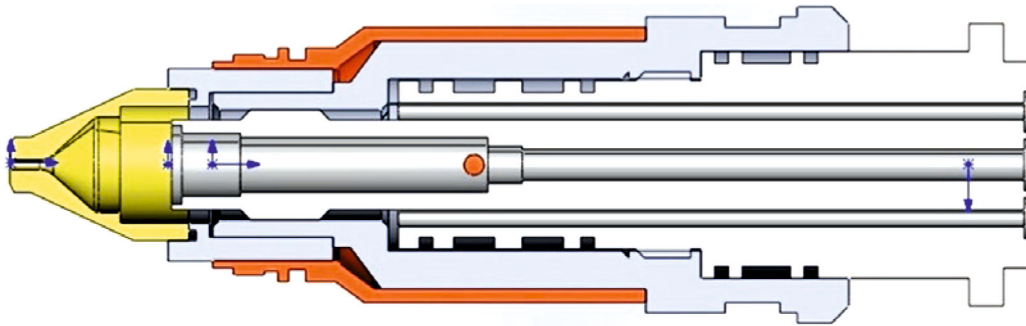

Fig. 2. PMVR-5.3 plasma torch for hugh-precision metal cutting (design diagram).

cial attention is paid to the development and adoption of Russian import-substituting plasma technologies and respective equipment the competitive advantages of which must be justified during their design as well as quality and efficiency tests.

FORMULATION OF THE PROBLEM

The upgrading of plasma technologies for cutting metallic materials has resulted in creating a new modification of plasma handling by narrow-jet plasma cutting, which has allowed considering it as an alternative to laser cutting in terms of precision and cutting quality [13−15]. The narrow-jet fifth-generation plasmatron PMVR-5.3 with a new gas swirling stabilization system of plasma arc has been designed and made by the authors at the premises of OOO Polygon SPA in the vein of such studies and considering their proper accumulated experience (Fig. 1).

This plasmatron is intended for the high-precision mechanized and manual plasma cutting of metals and has several design features significantly affecting the technology efficiency and quality. The overwhelming part of metal-cutting plasmatrons use the gas-dynamic stabilization system necessary for generating a plasma arc and protecting the plasmatron nozzle against its thermal influence, preventing the bypassing effect on the nozzle body and premature cathode wear. As a rule, a turbulence chamber is used for these pur-

poses; it is installed at the inlet of the nozzle unit with a variable flow cross-section that also ensures the gas-dynamic crimping of the plasma jet [16]. However, according to the authors' studies, most of these gas-swirling systems (GSS) do not allow achieving necessary maximal values and evenly distributing the gas-dynamic and thermal kinetic parameters of the gas-plasma flow (velocities, temperatures, specific consumption, energies) both, in the nozzle unit of the plasmatron and in the zone of the flow impact on the metal surface [17].

That is why air-plasma cutting often has an inferior quality in comparison with laser cutting used to cut steels of low thicknesses of up 10 mm and limited efficiency in comparison with gas cutting used to handle thick metal sheets. The efficiency of the GSS in the PMVR-5.3 plasmatron is improved using the symmetrical entry of plasma-generating gas (PGG) to the flow separation system, followed by supplying the PGG to the gas-dynamic flow stabilizer consisting of three tandem gas-air duct (GAD) elements: they are a gas-feed, a gas-generation, and a gas-swirling section using a generating and a stabilizing swirler with a variable number of swirling channels (Fig. 2).

The GAD design of the PMVR-5.3 plasmatron is optimized using the numerical analysis by the GSS gas-dynamic efficiency criteria.

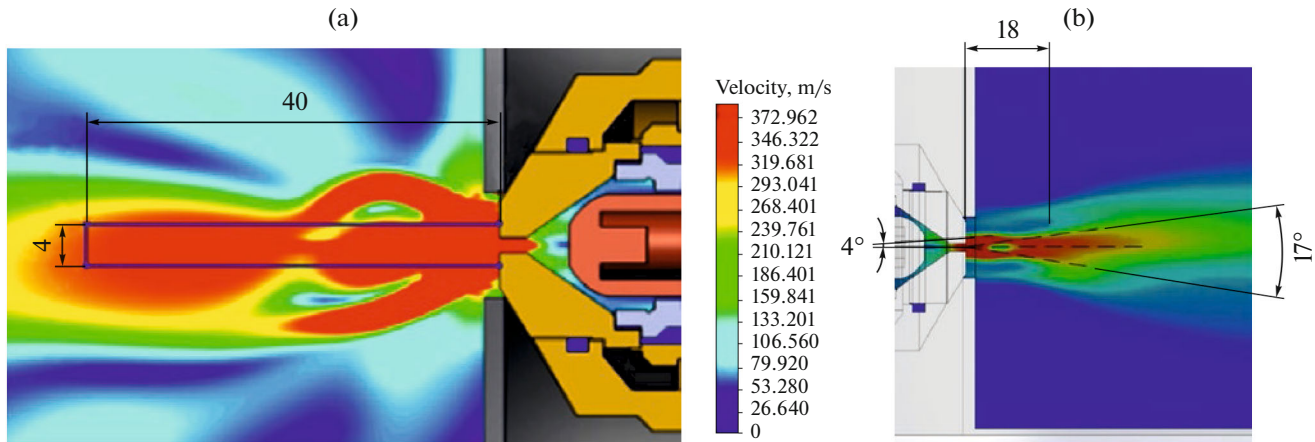In addition to determining specific dimensions of separate sections of the GAD, the most efficient tilts

Fig. 3. Calculation of plasma jet parameters for the PMVR-5.3 plasma torch: (a) the calculation scheme for the U-shaped trajectory; (b) the evaluation of the plasma jet geometry.

of the swirling channels were also determined (60–700 relative to the GAD axis) for achieving the best proportions of the axial and the tangential component of the PGG velocity that would be optimal for the specified structure and guarantee the maximal productivity and performance reliability. The efficiency of design at the initial stage was evaluated by numerical methods. See Fig. 3 for the design layout of determining the gas dynamic parameters of the plasma-arc flow and its configuration beyond the GAD of the plasmatron (including the zone of the impact on the cut metal surface).

As shown by the results of the gas dynamic analysis on the model (cold) jet that are represented in Figs. 3 and 4, the respective average and maximal velocities in the zone of the plasma-arc impact on the metal (butt end of the U-shaped trajectory 40 mm away from the plasmatron nozzle) increased by 60 and 30% at comparable input parameters in comparison with the parameters ensured by the currently popular PMVR-M plasmatron with the conventional GAD design with a nonsymmetrical PGG supply and a swirler in the GSS.

In this case, gas dynamic stabilization efficiency Z (percentage ratio of average linear deviation of parameters and their average value) increases by more than twofold. This efficiency characterizes the evenness of the distribution of gas dynamic characteristics (velocity in this calculation) in the control zone of the design trajectory:

$$Z = \frac{\sum_{i=1}^{n} \frac{|V_i - \bar{V}|}{n}}{\bar{V}} \times 100,$$

where $\bar{V}$ is the average velocity of the array of design velocities; n is the number of design points.

In addition, there is a reduction by 20–30% in the radial size of the kinetic core of the plasma jet

(Fig. 3b); this size is determined by the configuration of the zone of gas-plasma efflux with maximal velocities. It is essential that these conclusions can be also made in the other sections of the U-shaped control trajectory as well as in calculating other kinetic parameters (specific consumptions and energies) of the jet including the conditions of heating it with a plasma arc. It is obvious that the improvement in kinetic characteristics at a more even distribution of the gas-plasma flow parameters must significantly affect the improvement in the technology's efficiency, quality, and reliability.

STUDY METHOD

To confirm by experimentation the results of numerically analyzing the design efficiency of the PMVR-5.3 plasmatron, the cut quality and the struc-
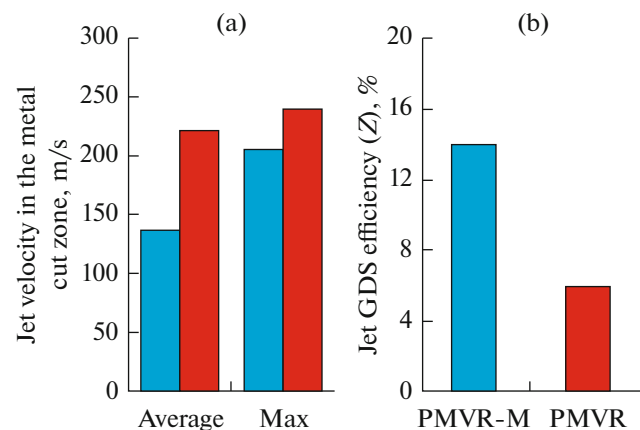

Fig. 4. Comparative analysis of velocities (a) and efficiency criterion of gas-dynamic stabilization Z (b) in the zone of the plasma jet impact on the metal: the blue bars are for PMVR-M; the red bars are for PMVR-5.3; (U-shaped trajectory—see Fig. 3, cold jet).

Table 1. Chemical composition of the studied steel, %

C	Si	Mn	P	S	Cr	Ni	Mo	Al
0.145	0.215	0.441	0.020	0.012	0.136	0.220	0.021	0.0088
Cu	Co	Ti	Nb	V	W	Pb	Mg	B
0.180	0.017	<0.0010	<0.0040	<0.0010	<0.0017	<0.0066	<0.0010	<0.0015
Sn	Zn	As	Bi	Ca	Ce	Zr	La	Fe
0.0083	<0.0020	0.015	0.012	0.0007	<0.0030	0.0025	<0.0010	98.5

turing kinetics of the thermal impact zone (TIZ) were studied at the narrow-jet high-precision air-plasma cutting of a thick-sheet steel band with a thickness of 40 mm. It should be noted that, in this case, precision is understood as the cut width and compliance with certain geometric characteristics of the cut surface. These characteristics are surface microtopography, angular tolerance (deviation), drossing in the bottom part of the cut and drippings in the top part as well as TIZ width the values of which are governed by GOST 14972–80 [18]. The results of the parametric analysis of plasma-arc cutting modes (current–voltage curve of the arc, burning efficiency, cutting velocity and productivity) allowed determining the optimal performance specifications of the plasmatron: cutting current of 120 A; cutting voltage of around 180 V; PGG pressure of around 4.5 atm; nozzle diameter of 1.9 mm; plasmatron sweep of 6–7 mm; cutting velocity of 0.3 m/min.

The structural tests were conducted under a NEO-PHOT-21 microscope at a magnification factor of 500 to 1000. The chemical composition of the steel sheets was determined by the spectral method on a SPEC-TROMAX device and averaged by burns in several points on the specimen cross-section surface. The potential variability in the data about the chemical composition of the test steel was identified by analyzing the concentration of all of the components in various randomly chosen sections across the sheet thickness. The distribution of chemical elements on the cut surface was determined by the microscale X-ray spectral analysis at a magnification factor of 2000; the analysis was made under a TESCAN VEGA IIXMU scanning electron microscope equipped with INCA ENERGY 450 energy dispersion analysis systems with an OXFORD ADD detector and INCA software. The surface microtopography of the cuts was tested with the help of a Veeco NT-1100 optical interferometer. The hardness value was determined on a LEICA device in the Materials Workstation software suite at a load of 25 and 1000 g on the top and bottom edge of the cut.

RESULTS AND DISCUSSION

For the results of analyzing the chemical composition of the tested steel for all of the chosen components

characterizing the grade composition of sheet materials, see Table 1.

According to GOST 380–2005 *Common quality carbon steel*, the test specimens can be identified as St3ps steel, with the mass fraction of the main components being within the tolerance limits of hot-rolled sheet products.

The visual analysis of the cut surface of the sheet exposed to plasma cutting in selected modes allowed determining the quality parameters and the configuration of the cut edges in case of using the considered plasmatron. According to external inspection (Fig. 5), in all of the tested sections, the macropattern of the cut along the specimen was almost identical and there were no traces of drossing and sticking of drops of the molten metal. In addition, there was no meltback and rounding of the top edge, which ensured an almost zero angular deviation of the cut encouraged by the maximal possible arc crimping during the narrow-jet air-plasma cutting of the materials. The absence of significant arc oscillation at the selected plasma cutting velocities is also a highly significant result, which has allowed achieving the minimal buckling of the cut line.

However, the buckled surface zone does not cover the entire cut surface and there are three distinct characteristic zones across the sheet thickness starting from the top edge. These zones are conditionally designated as smooth (Fig. 5, zone 1), intermediate (Fig. 5, zone 2), and buckled (Fig. 5, zone 3). They have different extension by width, and the buckled zone covers no more than 20% of the cut surface area on average. It is important to note that at the selected plasmatron performance parameters, the cut width along the entire handling length did not exceed 3 mm, which is well in line with the data in work [19].

It is known that during thermal cutting, a large temperature differential (from the melting to the starting temperature) is observed on a comparatively narrow section adjacent to the cut surface, which is caused by the fast movement of a concentrated heating source along the cut metal surface. As a result, metallurgical processes develop in the metal edges and are attended by changes in the chemical composition, structure, and mechanical properties in comparison with the original condition. That said, the structural
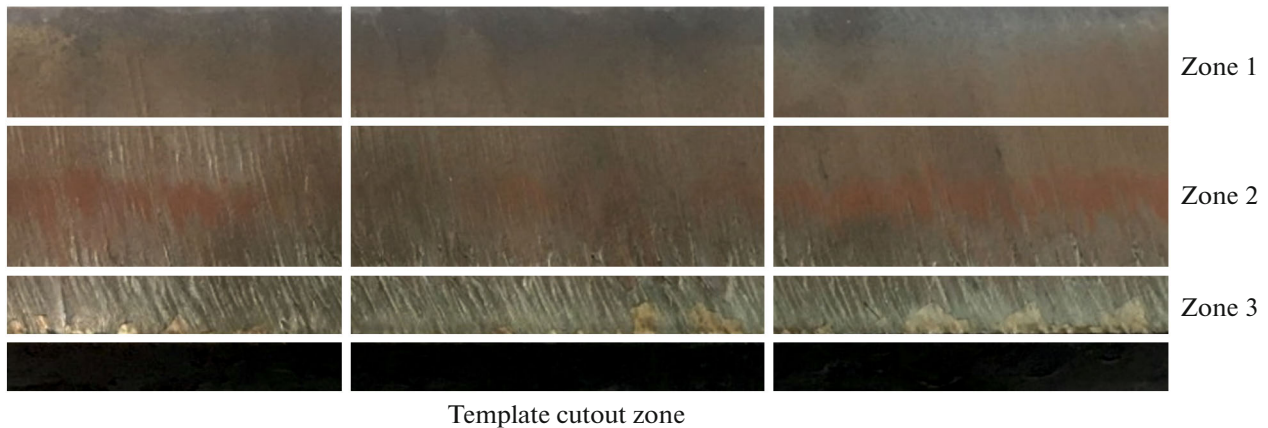
Zone 1

Zone 2

Zone 3

Template cutout zone

Fig. 5. Appearance of the plate cut surface after plasma treatment.
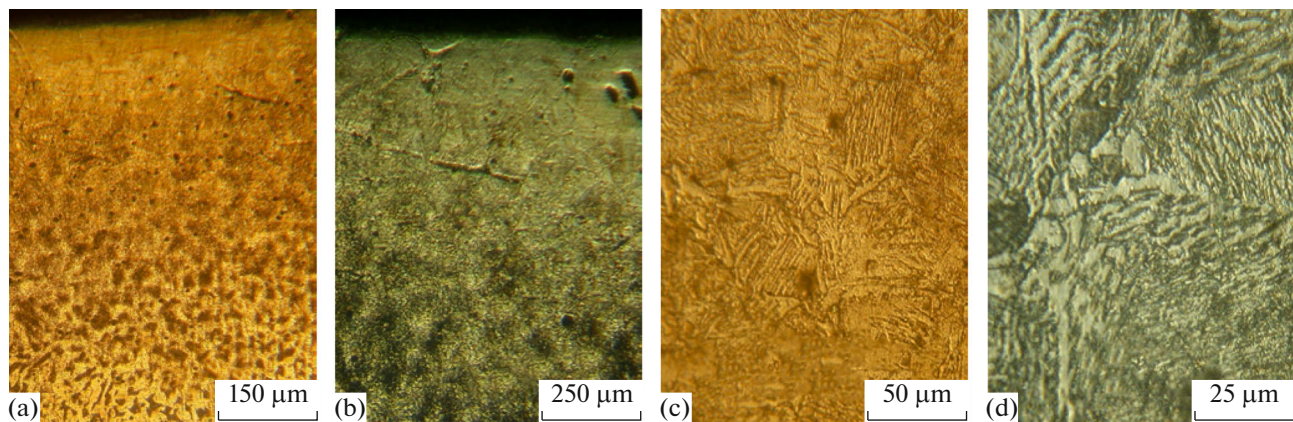

(a) 150 μm (b) 250 μm (c) 50 μm (d) 25 μm

Fig. 6. Microstructure of the near-surface layers of the tested steel depending on magnification factor.

transformations during the thermal cutting of metals are much different from the transformations during the conventional thermal treatment. In this case, the decomposition of solid solutions in the cutting zone progresses in more complex and continuously changing conditions, whereas in many cases the chemical heterogeneity in the thermal heating zone significantly changes the decomposition kinetics of solid solutions [20, 21]. As a consequence, the crystallization and structural transformations of the metal in the cut zone most often determine the subsequent processing and performance properties in this zone.

The microstructure of the near-surface layers of the tested steel after plasma cutting is shown at different magnification factors in Fig. 6.

In the considered case, special attention is drawn by the studies of the thermal processes in the cutting zone (thermal heating/melting). The structure and composition of the cutting zone influence the properties of the TIZ. As a result of thermal cutting, the generation of conditional sections was detected from the melting zone to the basic metal. On the whole, it can

be reckoned that the entire sectioning seam is a zone of thermal influence right to the original state of steel. The step-by-step hardness measurement with an interval of 50 μm starting from the top edge zone allowed determining the width of that zone, with its size depending on the chemical composition and thickness of the cut metal. In this case, according to the parametric conditions of the test, the width of that zone was determined as around 1000 μm (Fig. 7).

In terms of structural conditions, TIZ are divided in three subzones:

I is the critical overheating zone (COHZ) as a band of structureless martensite near the cut surface, where the temperatures are similar to melting temperatures;

II is the zone of heating to austenitic state, that is, phase recrystallization zone (PRCZ) with quenching structures;

III is the zone of heating to temperatures below the eutectoid conversion of steel in which transitional structures are generated, which is why this zone is known as transitional zone (TZ).
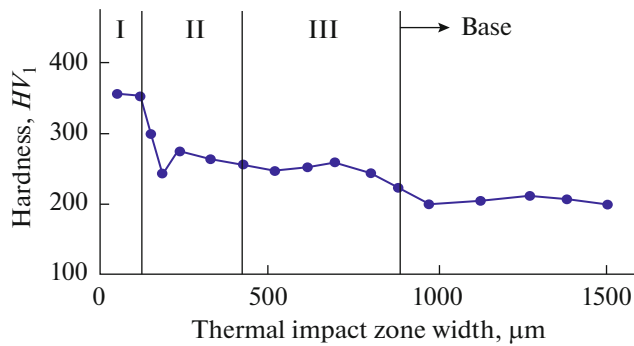
Fig. 7. Graph of hardness change over the width of the thermal impact zone.

The microstructural analysis allowed detecting significant changes in the structuring of TIZ subzones II and III in the test specimens. Thus, a nonetchable white layer of structureless martensite was generated on the cut surface in the COHZ, whereas a varied grain structure was generated in the PRCZ and TZ. A relatively low cutting rate of 0.3 m/min, selected for cutting out thick steel sheets, conditioned the structuring of 7-point enlarged grains of medium-lamellar perlite by recrystallization. That said, in the transitional subzone of the TZ, a sharp increase was registered in the amount of perlite in perlite-ferrite structure in comparison with the initial proportion in the steel base (Table 2).

These structuring features are largely determined by the redistribution of alloying elements in the test steel and, mainly, carbon during energy deposition. As shown by microscale X-ray structural analysis (Fig. 8), the diffusion redistribution of carbon significantly increased its concentration in the COHZ subzone; in the cut edge, that concentration was 0.76% (wt) at an averaged carbon concentration in the base of 0.14% (wt). It should be noted that, in the specified graph, the elements distribution diagram clearly shows an irregular distribution of carbon in various zones of the cut.

The carbon concentration is maximal in the meltback zone near the cut edge; in the PRCZ, this concentration decreases to 0.35−0.45% (wt) and evens closer to the end of the TZ in accordance with the chemical composition of the base. All of this fully reflects the morphology of the generated structures in various zones of the cut with an increasing distance from the edge. Also, according to the diagram, the meltback zone exhibits a significant reduction in the mass fraction of manganese and silicon in comparison with their initial levels as a result of intensive energy deposition in the cut zone by burnout.

Since these elements are constant process impurities in carbonous steel, their concentration is low and this reduction in their amount in the near-surface layers does not have any significant value. At the same time, the high carbon saturation of the surface layers sharply increased the hardness of the outer cut edges to a depth of 25 µm (Fig. 9). The intensive heat removal in this zone resulted in the self-tempering of the steel with the generation of an interlayer of structureless martensite to a depth of 10 µm. The compound under this interlayer to the end of the COHZ subzone is bainite structured as a highly dispersed ferrite-carbite mixture. It is important to point out that the bottom and top cut edges of thick steel sheets exhibit almost identical hardness distribution patterns, which is conditioned by the high efficiency of the GSS from the narrow-jet plasmatron during the entire period of gas-plasma exposure (within the thickness of the metal being cut).

During the quality evaluation of plasma cutting, much attention is paid to examining the surface for roughness in terms of the microgeometry of the cut line pattern. For the examination results, see Fig. 10 and Table 3. It is seen that the micropattern of the surface after plasma cutting is commensurate, by all of the

Table 2. Sample structure in subzones of thermal impact

Specimen thickness, mm	Zone	Zone thickness, mm	Structure
40	I (COHZ)	25	Structureless martensite
	II (PRCZ)	390	Medium-lamellar perlite, 7 points, interlamellar spacing below 1.20 µm
	III (TZ)	800	Perlite-ferritic structure with p/f ratio = 85/15
	Steel base	>1000	Perlite-ferritic structure with p/f ratio = 20/80

Table 3. Roughness of the cut surface

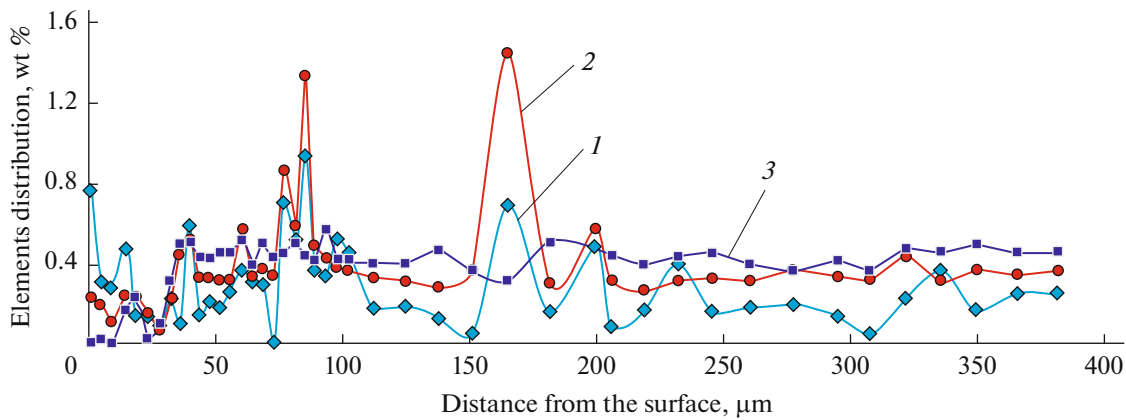| Type of treatment	Average roughness R_a, µm	Average square roughness R_a, µm	Absolute roughness $R_t(Rz)$, µm
Plasma cutting	21.94	26.69	171.61
GOST 2789-73 milling	20.00	25.00	160.00

Fig. 8. Distribution of alloying elements and carbon in the thermal impact zone (St3ps steel): (*1*) C; (*2*) Si; (*3*) Mn.
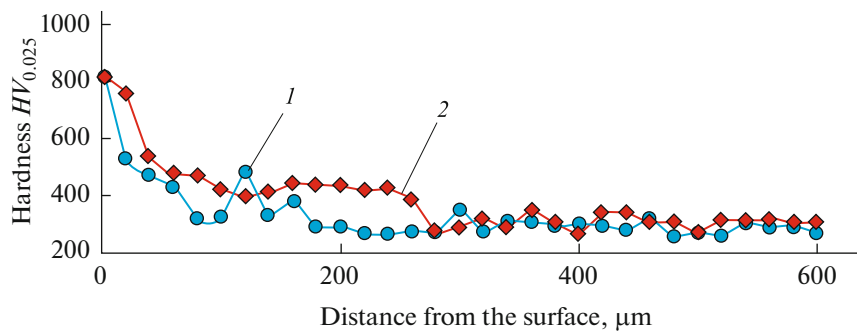

Fig. 9. Hardness distribution along the edges of the cut surface: (*1*) the lower edge; (*2*) the top edge.
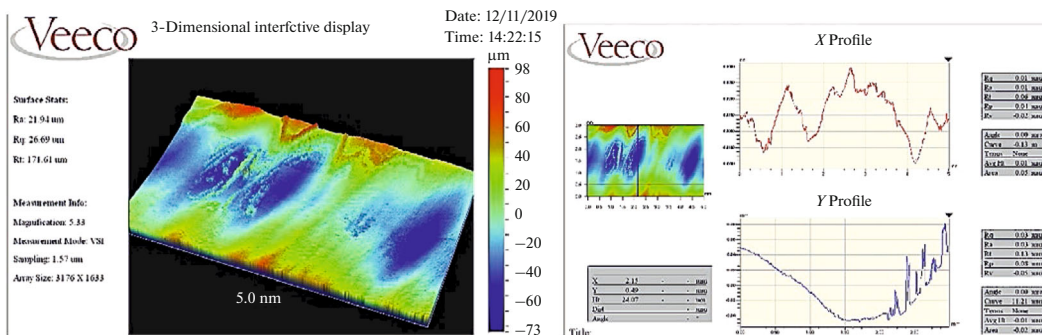

Fig. 10. Analysis of the surface relief after plasma cutting.

quality indicators, with the micropattern of the surface exposed to mechanical treatment after milling and corresponds to roughness class two by surface cleanliness.

CONCLUSIONS

According to the study results, it can be concluded that the engineering capabilities of the designed plasmatron PMVR-5.3, achieved using the new GSS system with two turbulence chambers and expansion chambers as well as symmetrical PFG supply allow performing a fairly high-quality cutting out of steel sheets during a narrow-jet air-plasma cutting in a fairly broad thickness range up to 40 mm and wider. However, it is necessary to consider than at large thicknesses a very extended TIZ is generated with significant structural changes in the main metal and changes in several other parameters. This is why blanks can be welded without preliminary mechanical machining at a cut width of no more than 20 mm; at large thick-

nesses the beveling from the cut surface is conducted at a minimal depth of 1 mm.

REFERENCES

1. Krink, V., Simler, H., and Laurisch, F., Plasmaschneidtechnologie—Erweiterung wirtschaftlicher Anwendungsgebiete, *ICCT 2006: Int. Schneidtechnische Tagung; Vorträge der gleichnamigen Konferenz*, Hannover, 2006, pp. 18−25.

2. Mussmann, J., Stand der Bearbeitung von ISO 4063:2009 "Schweissen und verwandte Prozesse—Liste der Prozesse und Ordnungsnummern," *Schweissen Schneiden*, 2010, nos. 7−8, pp. 430−433.

3. Krink, V., Plasmaschneiden − Ein vielseitiges Verfahren zum Schneiden dünner und dicker Bleche, *DVS Congress*, Nuremberg, 2010, pp. 73−78.

4. Esibyan, E.M., Air-plasma cutting: State and prospects, *Avtom. Svarka*, 2000, no. 12, pp. 6−20.

5. Antipov, N.A. and Medko, V.S., Determination of the defective surface layer during air-plasma cutting of blanks made of carbon low-alloy steel, *Elektrofiz. Elektrokhim. Metody Obrab.*, 2014, no. 2, pp. 25−27.

6. Vasiliev, A.N., Vnuk, V.V., Zinoviev, V.I., and Kotkina, T.V., Comparative study of air-plasma and plasma-arc cutting, *Izv. Mosk. Gos. Tekh. Univ.*, 2014, no. 2, pp. 13−18.

7. Gesteigerte Produktivität durch neueste Plasmaschneidtechnologie, *Schweissen Schneiden*, 2008, no. 9, pp. 458−459.

8. Nachbargauer, K., Mit Schneidhohmodus beim Plasmaschneiden reproduzierbare Schneidergebnisse erzeilen, *DVS Congress*, Nuremberg, 2010, pp. 95−96.

9. Wegmann, H., Gesthuysen, F.-J., and Holthaus, M., Plasma cutting—an economically viable process for mild and low-alloy steels, *Weld. Cutting*, 2005, vol. 4, no. 4, pp. 191−194.

10. Anakhov, S.V., *Printsipy i metody proektirovaniya plazmotronov* (Principles and Methods of Plasma Torches Design), Yekaterinburg: Ross. Gos. Profess.-Pedagog. Univ., 2018.

11. Conrads, H. and Schmidt, M., Plasma generation and plasma sources, *Plasma Sources Sci. Technol.*, 2000, vol. 9, no. 4, pp. 441−454.
https://doi.org/10.1088/0963-0252/9/4/301

12. Venkatramani, N., Industrial plasma torches and applications, *Curr. Sci.*, 2002, vol. 83, no. 3, pp. 254−262.

13. Loktionov, A.A., Assessment a cut of quality of sheet materials in the conditions of high-precision plasma cutting, *Obrab. Met.*, 2013, no. 4, pp. 85−89.

14. Rakhimyanov, H.M., Loktionov, A.A., and Nikitin, Yu.V., Evaluation of geometric precision cut of sheet materials with different high-precision plasma cutting technologies, *Obrab. Met.*, 2013, no. 3, pp. 25−30.

15. Kirkpatrick, I., High definition plasma—An alternative to laser technology, *Aircr. Eng. Aerosp. Technol.*, 1998, vol. 70, no. 3, pp. 215−217.
https://doi.org/10.1108/00022669810370349

16. Dresvin, S.V. and Zverev, S.G., *Plasmotrony. Konstruktsii, parametry, tekhnologii* (Plasma Torches: Designs, Parameters, Technologies), St. Petersburg: Izd-vo Politekh. Univ., 2010.

17. Anakhov, S.V., Pykin, Yu.A., and Matushkin, A.V., Improving the effectiveness of individual gaseous-vortex stabilization in plasma torches for precision cutting of metals, *Svar. Proizvod.*, 2019, no. 4, pp. 27−30.

18. *GOST* (State Standard) *14 792−80: Parts and blanks cut by oxygen and plasma arc cutting. Accuracy, quality of the cutting surface*, 1980.

19. Sukhorukov, N.V. and Smolentsev, E.V., Technology of plasma processing in materials separation, *Vestn. Voronezh. Gos. Tekh. Univ.*, 2009, vol. 5, no. 12, pp. 1−3.

20. Sumets, A.V. and Kassov, V.D., Regularities of structure formation of heat affected zone at metals cutting, *Vestn. Kharkov. Nats. Avtomobil.-Dorozhnii Univ.*, 2017, no. 77, pp. 166−170.

21. Lyashchenko, G.I., Quality in plasma-arc cutting, *Svarshchik*, 2012, no. 4, pp. 34−39.

Translated by S. Kuznetsov